

# Low-frequency spin dynamics as probed by $^{63}\text{Cu}$ and $^{199}\text{Hg}$ NMR in $\text{HgBa}_2\text{CuO}_{4+\delta}$ superconductors with different oxygen content

A. A. Gippius\*

*Faculty of Physics, Moscow State University, 119899 Moscow, Russia*

E. V. Antipov

*Faculty of Chemistry, Moscow State University, 119899 Moscow, Russia*

W. Hoffmann and K. Lüders

*Fachbereich Physik, Freie Universität Berlin, D-14195 Berlin, Germany*

G. Buntkowsky

*Fachbereich Organische Chemie, Freie Universität Berlin, D-14195 Berlin, Germany*

(Received 15 June 1998; revised manuscript received 9 September 1998)

$^{63}\text{Cu}$  and  $^{199}\text{Hg}$  nuclear magnetic resonance was performed on a series of powder  $\text{HgBa}_2\text{CuO}_{4+\delta}$  samples with different oxygen content  $\delta$  in order to study the influence of oxygen doping on the spin dynamics in the normal and superconducting state. The spin-lattice relaxation time  $T_1$  of  $^{199}\text{Hg}$  and  $^{63}\text{Cu}$  nuclei were measured over a wide range of temperature at different orientations of the crystallites with respect to the magnetic field. For the optimally doped sample ( $T_c=96$  K) we compared our experimental results to numerical calculations of the spin-lattice relaxation rate as a function of temperature below  $T_c$  for several types of the order parameter symmetry: isotropic  $s$  wave, anisotropic  $s$  wave without nodes,  $s$  wave with nodes, and  $d$  wave, using the different values of the gap parameter  $2\Delta/k_B T_c$  within the AF fluctuation model. The comparison with our experimental relaxation data shows that for  $^{199}\text{Hg}$  nuclei in the orientation  $\mathbf{B}_0 \parallel (a,b)$  plane as well as for  $^{63}\text{Cu}$  nuclei in both orientations,  $\mathbf{B}_0 \parallel (a,b)$  plane and  $\mathbf{B}_0 \parallel c$  axis, the experimental results are in coincidence with the  $d_{x^2-y^2}$ -wave symmetry with the gap parameter  $2\Delta/k_B T_c = 7.02$ . [S0163-1829(99)09801-X]

## I. INTRODUCTION

Spin dynamics in high-temperature superconductors has attracted much attention in recent years (see Refs. 1–3, for instance) since analyzing the relaxation characteristics can possibly shed light on the nature of the symmetry of the superconducting order parameter and the value and anisotropy of the energy gap. The reliable determination of these parameters is of considerable importance in understanding high-temperature superconductivity.

For the  $d_{x^2-y^2}$  pairing state the gap function  $\Delta(\mathbf{k}, T)$  may be presented in the form<sup>1</sup>

$$\Delta(\mathbf{k}, T) = \frac{1}{2} \Delta(T) (\cos k_x - \cos k_y), \quad (1)$$

where  $k_x$  and  $k_y$  are the  $x$  and  $y$  components of the wave vector  $\mathbf{k}$ , respectively. In  $\mathbf{k}$  space Eq. (1) describes a four-fold rotation symmetry pattern with two pairs of lobes which have an opposite sign. This sign change distinguishes a  $d$  state from an anisotropic  $s$  state [see Eqs. (8) and (9) in Sec. III C] where the gap function remains positive. Observations of a half-integer flux quantum by Kirtley *et al.*<sup>4</sup> as well as the quantum interference experiments on  $\text{YBa}_2\text{Cu}_3\text{O}_{7-\delta}$  crystals by Harlingen<sup>5</sup> are strong experimental evidence for the  $d$ -wave superconducting pairing state, which require a non-phonon mechanism of superconductivity.

The family of mercury cuprate superconductors  $\text{HgBa}_2\text{Ca}_{n-1}\text{Cu}_n\text{O}_{2n+2+\delta}$  has attracted attention due to extraordinary high transition temperatures  $T_c$ , which achieves 135 K for the  $n=3$  compound (Hg-1223). In comparison to

the Bi- and Tl-based superconductors the lattice-structures of Hg cuprates are practically free from distortions, such as incommensurate modulations, static displacements, cation substitutions, and superstructures. Because of these features the Hg-based superconductors, particularly the first member of the family  $\text{HgBa}_2\text{CuO}_{4+\delta}$  which has the simplest crystal structure containing only one type of  $\text{CuO}_2$  layer, are attractive objects for the fundamental study of the high- $T_c$  superconductivity phenomenon. In spite of the intensive study, however, the fundamental understanding concerning the mechanism of superconductivity is still the subject of controversial discussions. Reliable energy gap values and its symmetry have not yet been obtained<sup>6,7</sup> and the question of  $s$ - or  $d$ -wave pairing has not been convincingly answered.<sup>2</sup>

NMR is a sensitive method for the study of low-frequency spin dynamics in both the normal and the superconducting state in  $\text{HgBa}_2\text{CuO}_{4+\delta}$  and other high- $T_c$  superconductors, especially through the studies of the Knight shift and spin-lattice relaxation.<sup>1-3,8</sup> In this paper we present  $^{63}\text{Cu}$  and  $^{199}\text{Hg}$  NMR performed on a series of powder  $\text{HgBa}_2\text{CuO}_{4+\delta}$  samples with different oxygen content  $\delta$ .

## II. PREPARATION AND EXPERIMENTAL DETAILS

For the NMR measurements we used the same series of  $\text{HgBa}_2\text{CuO}_{4+\delta}$  powder samples with different content which has been earlier studied by nuclear quadrupole resonance (NQR).<sup>9</sup> The details of the synthesis are described in Ref. 10. After the initial preparation step the samples were annealed in order to change the doping level. The following samples were used.

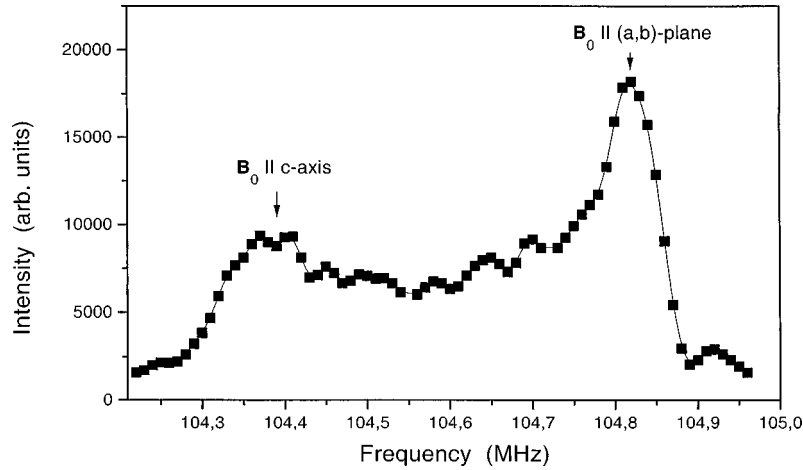


FIG. 1.  $^{199}\text{Hg}$  powder NMR spectrum of the sample No. 3 measured at  $T=90$  K. The singularities of the spectrum corresponding to the different magnetic field orientations are shown by the arrows.

No. 1: annealed in vacuum at  $345^\circ\text{C}$ ,  $\delta=0.015(5)$ ,  $T_c=39(2)$  K.

No. 2: annealed in vacuum at  $300^\circ\text{C}$ ,  $\delta=0.02(1)$ ,  $T_c=70(2)$  K.

No. 3: annealed in Ar at  $350^\circ\text{C}$ ,  $\delta=0.02(1)$ ,  $T_c=72(2)$  K.

No. 4: as prepared,  $\delta=0.06(1)$ ,  $T_c=95(2)$  K.

No. 5: annealed in oxygen flow,  $\delta=0.08(1)$ ,  $T_c=96(2)$  K.

No. 6: annealed in  $\text{O}_2$  at  $250^\circ\text{C}$  (100 bar),  $\delta=0.09(1)$ ,  $T_c=89(2)$  K.

No. 7: prepared under high pressure according to the technique described in Ref. 11,  $\delta=0.14(2)$ , not superconducting.

All samples were single phase compounds as characterized by the x-ray powder diffraction technique. The extra oxygen content  $\delta$  was determined by iodometric titration.<sup>12</sup> The ac magnetization curves as well as the structural parameters of the samples have been presented in Ref. 9 (Fig. 2 and Table 1).

The  $^{63}\text{Cu}$  and  $^{199}\text{Hg}$  NMR spectra were measured using a point-by-point Hahn spin-echo technique at a magnetic field of  $B_0=13.8$  T using full 32-phase cycling sequence to avoid echo distortions from the free induction decay (FID) and ringing. This sequence was repeated 10 times at each frequency point. The spin-lattice relaxation rates were measured using the saturation recovery method at the spectral positions corresponding to the  $\mathbf{B}_0 \perp (a,b)$  plane and  $\mathbf{B}_0 \parallel (a,b)$  plane in the temperature range of 4.2–300 K.

To minimize the error in the  $T_1$  determination due to the excitation of neighboring regions of the spectrum we used a relatively long  $\pi/2$  pulse of  $10 \mu\text{s}$  pulse length which corresponds to an excitation bandwidth of approximately 100 kHz. The shift values of  $^{63}\text{Cu}$  were calculated in respect to the resonance frequency of the bare core of  $^{63}\text{Cu}$  with the gyromagnetic ratio  $^{63}\gamma=11.2845 \text{ MHz/T}$ .<sup>13</sup>

### III. RESULTS AND DISCUSSION

#### A. The $^{199}\text{Hg}$ spectra and spin-lattice relaxation

The typical  $^{199}\text{Hg}$  spectrum of  $\text{HgBa}_2\text{CuO}_{4+\delta}$  shown in Fig. 1 exhibits the powder-pattern line shape which corresponds to an  $I=\frac{1}{2}$  nuclei in the presence of an axial-

symmetric anisotropic shift tensor (chemical and Knight shift) in the first order of perturbation theory. This line shape corresponds to the linear “dumbbell” coordination of Hg and O atoms along the  $c$  axis. Almost no influence of the oxygen content  $\delta$  on the  $^{199}\text{Hg}$  spectral shape and width has been found in the temperature range of 4–300 K which can be attributed to a relatively small change of the local structural arrangement of the  $\text{Hg}^{2+}$  cations with oxygen doping. As has been mentioned earlier by Suh *et al.*<sup>14</sup> and Horvatić *et al.*,<sup>15</sup> the resolution of NMR measurements on randomly oriented powder samples is not high enough to registrate any reliable temperature dependence of  $^{199}\text{Hg}$  Knight shift. The spin-lattice relaxation measurements were performed at the position of the spectral maximum at the  $\mathbf{B}_0 \parallel (a,b)$  plane. The recovery of the magnetization in the measured temperature range 4.2–300 K is monoexponential for all samples. In comparison to the spin-lattice relaxation of  $^{63}\text{Cu}$  the spin-lattice relaxation time of  $^{199}\text{Hg}$  is in one order of magnitude longer. This difference can be attributed to the relatively weak hyperfine coupling of  $^{199}\text{Hg}$  nuclei to the  $\text{CuO}_2$  layers.

The resulting temperature dependences of the  $(T_1 T)^{-1}$  product for the samples 3–7 are shown in Fig. 2. The non-superconducting overdoped sample No. 7 shows a Korringa behavior with  $(T_1 T)^{-1}=0.13 \pm 0.02 \text{ s}^{-1} \text{ K}^{-1}$ . For the optimally doped sample No. 5 the  $(T_1 T)^{-1}$  product is also almost constant above  $T_c$  with the value of  $0.1 \text{ s}^{-1} \text{ K}^{-1}$  which is in a good agreement with the results of Suh *et al.* for the nonoriented and oriented Hg-1201 powder samples with the  $T_c$  value of 95 K (Ref. 14) and 96 K (Ref. 16), respectively. By careful study of Fig. 2 one can detect that for the overdoped sample No. 6 the  $(T_1 T)^{-1}$  slightly decreases with temperature in the vicinity of  $0.1 \text{ s}^{-1} \text{ K}^{-1}$  above  $T_c$  while the underdoped samples No. 3 and No. 4 show slight monotonic increase near the same value. Such deviation from the Korringa behavior above  $T_c$  in the overdoped regime shows that  $(T_1 T)^{-1}$  for  $^{199}\text{Hg}$  is affected by antiferromagnetic (AF) spin fluctuations which are peaked at the AF wave vector  $Q_{\text{AF}}=(\pi/a, \pi/a)$ . In the case of long correlated 3D AF interactions involving neighboring  $\text{CuO}_2$  layers this contribution should be completely vanished at the Hg site due to form factor  $^{199}\text{F}(Q_{\text{AF}})=0$  determined by the symmetry of linear coordination Cu-O-Hg-O-Cu along the  $c$  axis.<sup>17</sup> Our

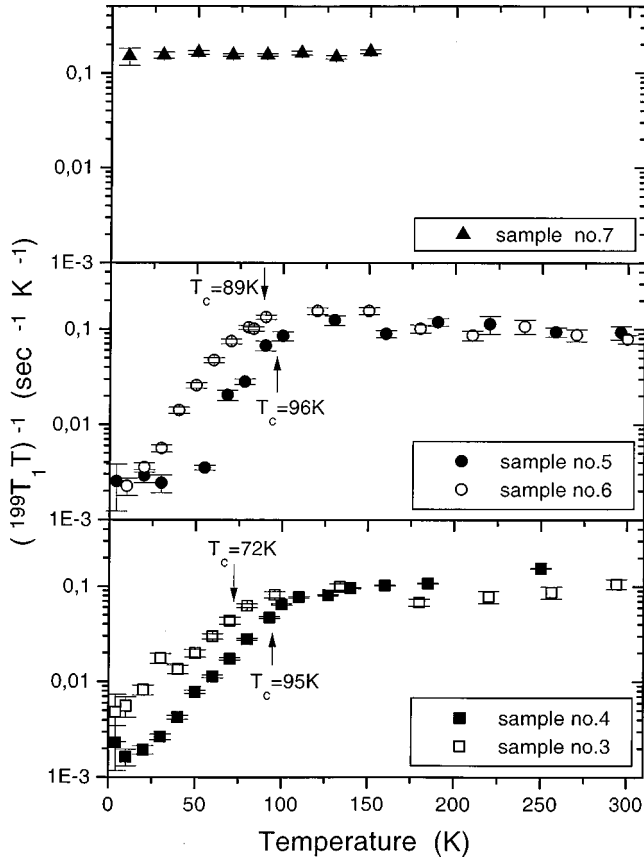


FIG. 2. Temperature dependences of  $^{199}\text{Hg}$  spin-lattice relaxation product  $(T_1T)^{-1}$  for the  $\text{HgBa}_2\text{CuO}_{4+\delta}$  samples Nos. 3–7. The corresponding  $T_c$  values are shown by the arrows.

result shows that this filtering is not perfect and there is a fluctuating transferred hyperfine field at Hg sites. A similar effect has been found earlier by Horvatić *et al.* for  $^{17}\text{O}$  in overdoped  $\text{YBa}_{1.52}\text{Sr}_{0.08}\text{Cu}_3\text{O}_7$  (Ref. 18) and Julien *et al.* for  $^{199}\text{Hg}$  in overdoped  $\text{HgBa}_2\text{CaCu}_2\text{O}_{6+\delta}$ .<sup>19</sup> Below  $T_c$  the temperature dependence of the relaxation rate for the samples 3–6 shows deviations from BCS-like behavior which will be discussed in Sec. III C.

### B. $^{63}\text{Cu}$ spectra and spin-lattice relaxation in $\text{HgBa}_2\text{CuO}_{4+\delta}$

The typical room temperature  $^{63}\text{Cu}$  spectra ( $-\frac{1}{2} \leftrightarrow \frac{1}{2}$  central transition) of  $\text{HgBa}_2\text{CuO}_{4+\delta}$  with different oxygen content are presented in Fig. 3. The powder line shape of the spectra is the superposition of the anisotropic chemical and Knight shift broadened by the quadrupole interaction in the second order of perturbation theory.<sup>20</sup> The influence of the quadrupole interaction on the spectral width and shape is rather strong. Our previous NQR study performed on the same series of  $\text{HgBa}_2\text{CuO}_{4+\delta}$  samples has shown that the copper quadrupole frequency  $^{63}\nu_Q$  significantly and monotonically increases with increasing oxygen content  $\delta$ .<sup>9</sup> The line shape is also essentially affected by the orientation effect which partially aligns the crystallites in the direction  $\mathbf{B}_0 \parallel c$  at  $T > T_c$  and the  $\mathbf{B}_0 \parallel (a, b)$  plane at  $T < T_c$ .<sup>21</sup> The powder spectra were simulated by numerical integration of the single crystal resonance frequency value  $\nu_{-1/2 \leftrightarrow 1/2}$  [Eq. (10) from Ref. 20] over the spherical surface with  $64 \times 64$  points using the asymmetry parameter  $\eta = 0$  and the copper quadrupole

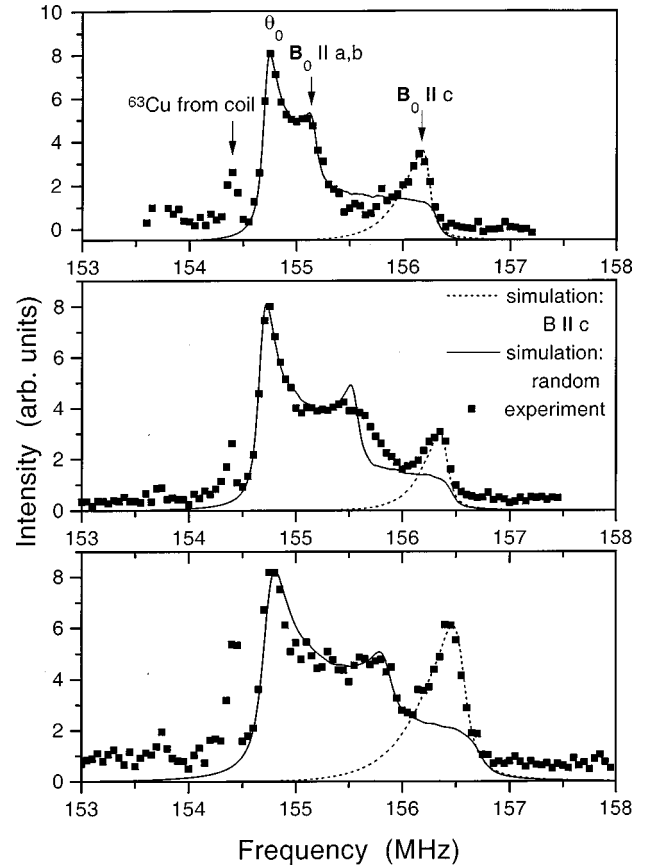


FIG. 3.  $^{63}\text{Cu}$  powder NMR spectra for the samples No. 3 (upper), No. 5 (middle), and No. 6 (down) measured at room temperature. Only the central transitions  $-\frac{1}{2} \leftrightarrow \frac{1}{2}$  are presented. The left singularity corresponds to the angle  $\theta_0 = 60.15^\circ$  between the magnetic field  $\mathbf{B}_0$  and the  $c$  axis (Ref. 20). The spectra simulation has been performed for the case of statistical distribution of powder crystallite orientation to the  $\mathbf{B}_0$  (solid line) as well as for  $\mathbf{B}_0 \parallel c$  orientation (dashed line).

frequency values  $^{63}\nu_Q$  obtained from the NQR measurements.<sup>9</sup> The calculations were fitted to the experimental spectra. From this procedure the principle values of the total shift tensor  $K_{xx,yy} = K_\perp$  and  $K_{zz} = K_\parallel$  in the dependence on temperature were determined. The results are presented in Fig. 4. Using the observed values of  $K_\parallel$  and  $K_\perp$  one can determine the isotropic  $K_{\text{iso}}$  and anisotropic  $K_{ax}$  parts of the total shift:

$$K_{\text{iso}} = 1/3(K_\parallel + 2K_\perp),$$

$$K_{ax} = 1/3(K_\parallel - K_\perp). \quad (2)$$

The observed shift  $K(T)$  in general, consists of the orbital, spin, and diamagnetic terms:

$$K(T) = K_{\text{orb}} + K_{\text{spin}}(T) + K_{\text{dia}}(T), \quad (3)$$

where the temperature-independent orbital shift includes the Van Vleck term  $K_{\nu\nu}$  and the chemical shift  $\delta$

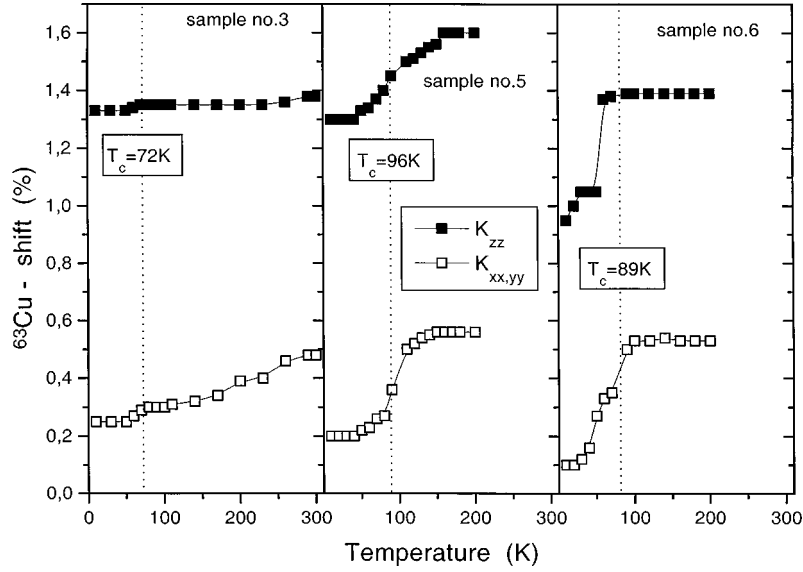


FIG. 4.  $^{63}\text{Cu}$  Knight shift of the different  $\text{HgBa}_2\text{CuO}_{4+\delta}$  samples in dependence on temperature.

$$K_{\text{orb}} = K_{\text{vv}} + \delta,$$

$$K_{\text{dia}}(T) = 4\pi(1-N)\frac{M(T,B)}{B}. \quad (4)$$

Here  $M(T,B)$  is the magnetization of the sample in the magnetic field  $B$ ,  $N$  is the demagnetization factor. In  $\text{HgBa}_2\text{CuO}_{4+\delta}$  the diamagnetic term arises only below  $T_c$  and is considered to be of an order of 0.01% (Ref. 16) which is rather small compared to the two other terms in Eq. (3). Following the Yosida model<sup>22</sup> we consider  $K_{\text{spin}} \rightarrow 0$  for  $T \rightarrow 0$  and extract the components of the total shift for different samples of  $\text{HgBa}_2\text{CuO}_{4+\delta}$  taken at 200 and 20 K. The results are listed in Table I. As follows from Table I, there is a strong dependence of the copper shift components on the oxygen doping level  $\delta$ . The isotropic part of the spin term  $K_{\text{spin}}^{\text{iso}}$ , which is proportional to the spin susceptibility exhibits a significant and monotonic increase with increasing  $\delta$  from the underdoped sample No. 3 to the overdoped sample No. 6. The ratio of the  $K_{\text{spin}}^{\text{iso}}$  values for these three samples is 1:3.4:4.3 which is in a good coincidence with the ratio 1:4:4.5 of the oxygen content  $\delta$  and the hole number  $2\delta$  in these samples.

As in other high-temperature superconductors (HTSC's) (Y, Tl HTSC's)<sup>17,23</sup> the main mechanism of the spin-lattice relaxation in  $\text{HgBa}_2\text{CuO}_{4+\delta}$  is the magnetic relaxation caused by the electron spin fluctuations in the Cu-O layers.

In contrast to the  $^{199}\text{Hg}$   $T_1$  measurements the observed  $^{63}\text{Cu}$  recovery curve for the  $-\frac{1}{2} \leftrightarrow \frac{1}{2}$  central transition is not monoexponential because of the influence of the satellite transitions  $-\frac{3}{2} \leftrightarrow -\frac{1}{2}$  and  $\frac{1}{2} \leftrightarrow \frac{3}{2}$  which are not saturated by the applied saturation pulse sequence. Taking into account this influence we used a biexponential function according to<sup>24</sup>

$$I(t) = I_{\infty} \left( 1 - \frac{2}{5} e^{-2t/T_1} - \frac{3}{5} e^{-12t/T_1} \right) \quad (5)$$

which gives a very good fit to the experimental recovery curves (Fig. 5). The extracted  $T_1$  values in dependence on temperature for the samples No. 3 and No. 6 are presented in Fig. 6. The underdoped sample No. 3 shows a gradual increase of the  $(T_1 T)^{-1}$  product with temperature above  $T_c$  while the overdoped sample No. 6 ( $T_c = 89$  K) exhibits a broad maximum at around 90–100 K and then decreases with increasing temperature. Such a doping dependence of the copper spin-lattice relaxation behavior due to the temperature-dependent AF spin fluctuation above  $T_c$  is the characteristic feature of the layered cuprate superconductors (see, for instance Refs. 8, 17, and 23).

### C. Comparison with the theoretical model

The temperature dependences of the spin-lattice relaxation rate have been numerically calculated using the effective random phase approximation (RPA) developed in Refs.

TABLE I. Components of the total shift for the  $^{63}\text{Cu}$  ( $-\frac{1}{2} \leftrightarrow \frac{1}{2}$ ) central transition for  $\text{HgBa}_2\text{CuO}_{4+\delta}$  samples with different oxygen content  $\delta$  at  $T=200$  K and  $T=20$  K.

Sample No.	Oxygen content $\delta$ $\pm 0.01$	$K_{xx,yy}$ (%)	$K_{zz}$ (%)	$K_{xx,yy}$ (%)	$K_{zz}$ (%)	$K_{\text{spin}}^{\text{iso}}$ (%)
		$\pm 0.05$ $T=200$ K	$\pm 0.05$ $T=200$ K	$\pm 0.05$ $T=20$ K	$\pm 0.05$ $T=20$ K	$\pm 0.08$ $T=200$ K
3	0.02	0.39	1.35	0.25	1.33	0.10
5	0.08	0.56	1.60	0.20	1.30	0.34
6	0.09	0.53	1.39	0.10	0.95	0.43

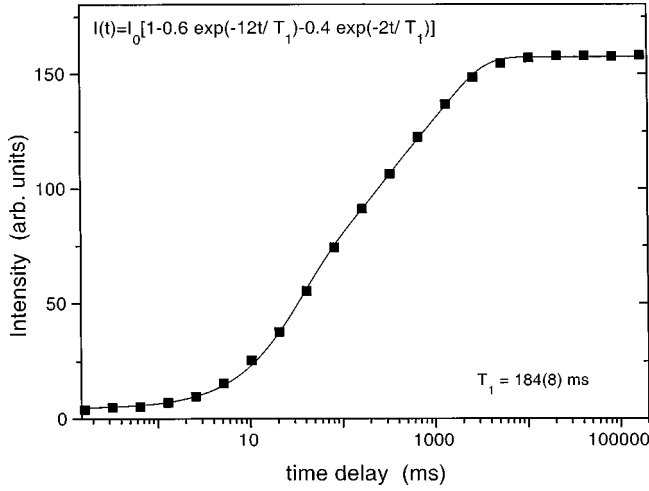


FIG. 5.  $^{63}\text{Cu}$  magnetization recovery curve for the sample No. 5 measured at  $T=10$  K. The solid line is the best fit of the experimental data by a double exponential function [Eq. (5)].

25–30 as quantitative theoretical model for the dynamical spin susceptibility. In the normal as well as in the superconducting state it has been shown that a RPA form for the electronic spin susceptibility  $\chi(\omega)$  can be adjusted to give a reasonable quantitative fit to the NMR data.<sup>26–31</sup> The details of calculations will be published elsewhere.

The superconducting gap function  $\Delta_k = \Delta(T) \phi_k$  consists of a temperature-dependent amplitude  $\Delta(T)$  and a  $T$ -independent momentum dependence characterized by the normalized function  $\phi_k$ . Following Ref. 29, the temperature dependence of the amplitude is described by the analytic expression

$$\Delta(T) = \Delta(0) \tanh(\alpha \sqrt{T_c/T - 1}), \quad (6)$$

where  $\alpha$  characterizes the sharpness of the drop off of  $\Delta(T)$ . Since the actual value of  $\alpha$  is only of minor significance for the final results on the spin susceptibility, the value  $\alpha=2.2$  of Ref. 29 has been used. The remaining open parameter for the characterization of the gap amplitude is the zero temperature gap  $\Delta_0$  or alternatively the ratio  $2\Delta_0/k_B T_c$ . Finally, for the characterization of the  $\mathbf{k}$  dependence of the gap function the following different scenarios have been investigated:

$$\phi_k^{s,\text{iso}} = 1 \quad (7)$$

for the isotropic  $s$  wave,

$$\phi_k^{s1,\text{ext}} = \frac{1}{6} + \frac{5}{96} (\cos k_x - \cos k_y)^4 \quad (8)$$

as extended  $s$  wave with minimum gap  $\Delta_{\min} = 1/6\Delta(T)$ ,

$$\phi_k^{s2,\text{ext}} = \frac{1}{2} (\cos k_x - \cos k_y)^2 \quad (9)$$

as extended  $s$  wave with nodes and finally

$$\phi_k^d = \frac{1}{2} (\cos k_x - \cos k_y) \quad (10)$$

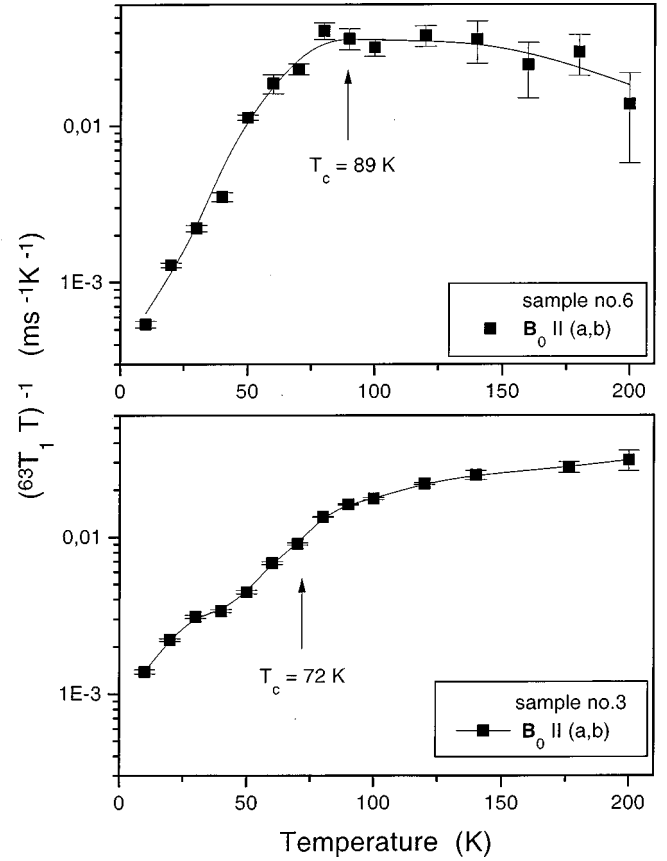


FIG. 6.  $^{63}\text{Cu}$  spin-lattice relaxation product  $(T_1 T)^{-1}$  for the  $\text{HgBa}_2\text{CuO}_{4+\delta}$  samples No. 3 and No. 6 in dependence on temperature. The corresponding  $T_c$  values are shown by the arrows. The solid lines are just guides for the eye.

for the  $d$ -wave state which is believed to be the relevant symmetry of a spin-fluctuation induced pairing state. Note, the common feature of all the momentum-dependent gap functions is that, in agreement with the angle-resolved photoemission experiments,<sup>32</sup> the gap maximum is located near the  $(\pi, 0)$  point of the Brillouin zone.

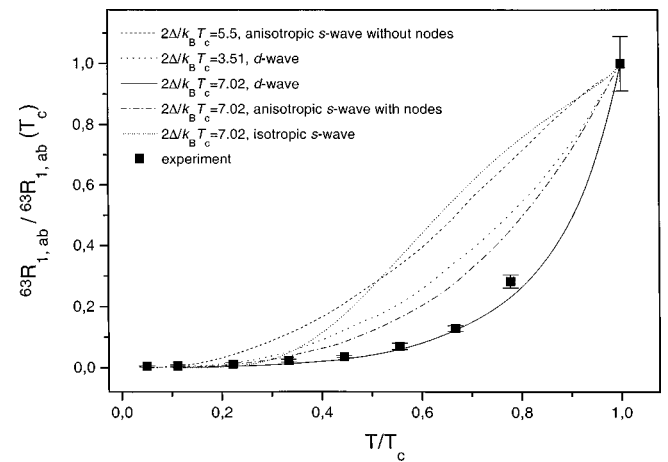


FIG. 7. Normalized  $^{63}\text{Cu}$  spin-lattice relaxation rate in the orientation  $\mathbf{B}_0 \parallel (a,b)$  plane for the sample No. 5 in dependence on temperature below  $T_c$ . The numerical calculations for different symmetries of the order parameter and different  $2\Delta/k_B T_c$  values are presented.

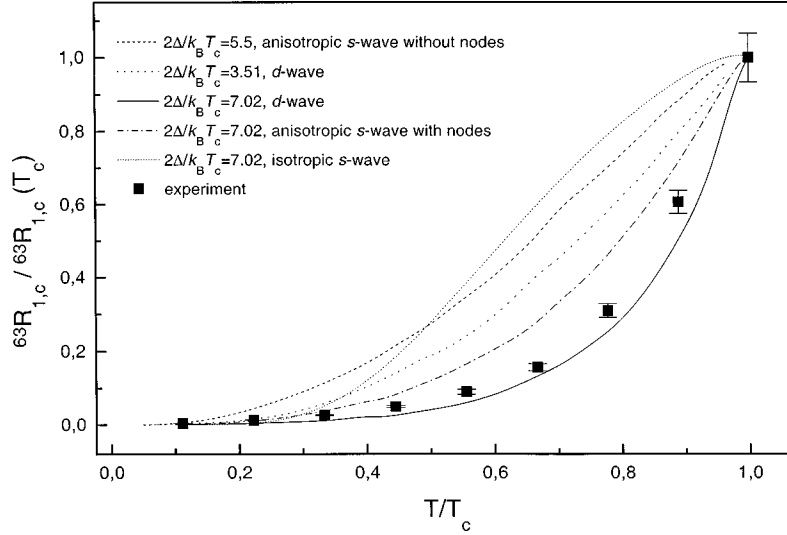


FIG. 8. Normalized  $^{63}\text{Cu}$  spin-lattice relaxation rate in the orientation  $\mathbf{B}_0 \parallel c$  axis for the sample No. 5 in dependence on temperature below  $T_c$ . The numerical calculations for different symmetries of the order parameter and different  $2\Delta/k_B T_c$  values are presented.

The calculations have been performed for  $^{199}\text{Hg}$  and  $^{63}\text{Cu}$  nuclei below  $T_c$  for the optimally doped sample No. 5. The resulting curves were compared with the experimentally obtained temperature dependences of the  $^{199}\text{Hg}$  and  $^{63}\text{Cu}$  spin-lattice relaxation rate normalized to the corresponding value at  $T=T_c$  and are presented in Figs. 7–9. As it follows from Figs. 7–9 for  $^{199}\text{Hg}$  nuclei in the orientation  $\mathbf{B}_0 \parallel (a, b)$  plane as well as for  $^{63}\text{Cu}$  nuclei in both orientations the experimental results are best described by the  $d_{x^2-y^2}$ -wave symmetry assuming the gap parameter  $2\Delta/k_B T_c = 7.02$ .

#### IV. SUMMARY

We have measured the NMR spectra and spin-lattice relaxation rate of  $^{63}\text{Cu}$  and  $^{199}\text{Hg}$  nuclei in the temperature range of 4.2–300 K for the series of  $\text{HgBa}_2\text{CuO}_{4+\delta}$  samples with different oxygen content. The  $^{199}\text{Hg}$  spin-lattice relaxation for the strongly overdoped nonsuperconducting sample

No. 7 and for the optimal doped sample No. 5 exhibits a Korringa behavior with  $(^{199}T_1 T)^{-1} = 0.13$  and  $0.1 \text{ s}^{-1} \text{ K}^{-1}$ , respectively. For the overdoped sample No. 6 the  $(T_1 T)^{-1}$  slightly decreases with temperature in the vicinity of  $0.1 \text{ s}^{-1} \text{ K}^{-1}$  above  $T_c$  while the underdoped samples No. 3 and No. 4 show slight monotonic increase near the same value. This result shows that at Hg sites the filtering of AF spin fluctuations peaked at  $Q_{\text{AF}} = (\pi/a, \pi/a)$  is not perfect and there is a fluctuating transferred hyperfine field at mercury sites.

The temperature behavior of the  $^{63}\text{Cu}$  spin-lattice relaxation rate above  $T_c$  in dependence on the doping level is typical for copper oxide HTSC's: the underdoped sample No. 3 shows the gradual increase of the product  $(T_1 T)^{-1}$  with temperature above  $T_c$  while the overdoped sample No. 6 exhibits a broad maximum at around  $T=100 \text{ K}$ . For the optimally doped  $\text{HgBa}_2\text{CuO}_{4+\delta}$  compound the temperature

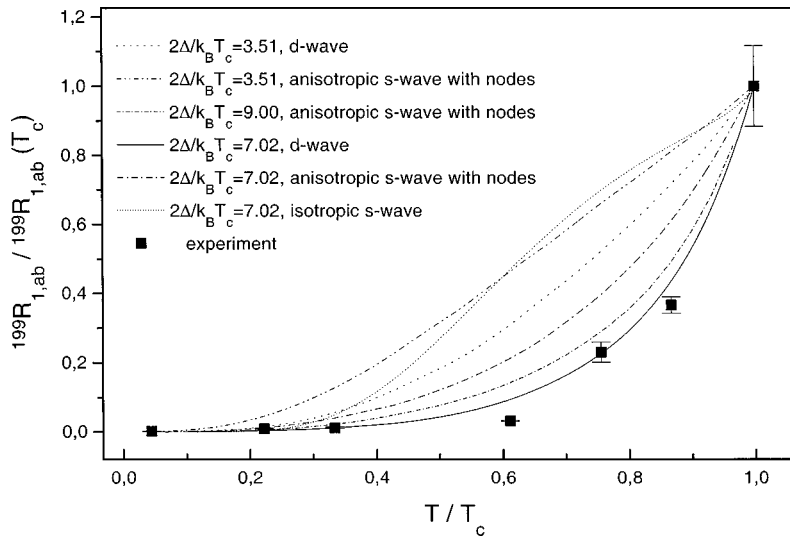


FIG. 9. Normalized  $^{199}\text{Hg}$  spin-lattice relaxation rate in the orientation  $\mathbf{B}_0 \parallel (a, b)$  plane for the sample No. 5 in dependence on temperature below  $T_c$ . The numerical calculations for different symmetries of the order parameter and different  $2\Delta/k_B T_c$  values are presented.

dependences of the spin-lattice relaxation rates below  $T_c$  have been numerically calculated for different types of the order parameter symmetry: isotropic  $s$  wave, anisotropic  $s$  wave without nodes,  $s$  wave with nodes, and  $d$  wave, using different values of the gap parameter  $2\Delta/k_B T_c$  within the AF fluctuation model. The comparison with our experimental relaxation data shows that for  $^{199}\text{Hg}$  nuclei in the orientation  $\mathbf{B}_0 \parallel (a, b)$  plane as well as for  $^{63}\text{Cu}$  nuclei in both orientations the experimental results are best described by the

$d_{x^2-y^2}$ -wave symmetry with the gap parameter  $2\Delta/k_B T_c = 7.02$ .

#### ACKNOWLEDGMENTS

The authors express their special gratitude to J. Schmalian, K. Kunze, and K. H. Bennemann for performing the numerical calculations of  $(T_1 T)^{-1}$  vs  $T$  behavior, help in theoretical aspects, and many fruitful discussions. This work was supported by the ‘‘Volkswagen Stiftung, Federal Republic of Germany,’’ Grant No. 1/73680.

\*Corresponding author. FAX: 007-095-3625576; electronic address: gippius@lt228.phys.msu.su

<sup>1</sup>N. Bulut and D. J. Scalapino, Phys. Rev. Lett. **68**, 706 (1992).

<sup>2</sup>A. Sudbo, S. Chakravarty, S. Strong, and P. W. Anderson, Phys. Rev. B **49**, 12 245 (1994).

<sup>3</sup>D. M. Thelen and D. Pines, Phys. Rev. B **49**, 3528 (1994).

<sup>4</sup>J. P. Kirtley, C. C. Tsuei, M. Rupp, J. Z. Sun, Lock See Yuhannes, A. Gupta, M. B. Ketchen, K. A. Moler, and M. Bhushan, Phys. Rev. Lett. **76**, 1336 (1996).

<sup>5</sup>D. J. Van Harlingen, Rev. Mod. Phys. **67**, 515 (1995).

<sup>6</sup>C. Rossel, R. R. Schulz, A. Schilling, H. R. Ott, and J. Karpinsky, Physica C **235-240**, 1871 (1994).

<sup>7</sup>J. Chen, J. F. Zasadzinski, K. E. Gray, J. L. Wagner, and D. G. Hinks, Phys. Rev. B **49**, 3683 (1994).

<sup>8</sup>H. Yasuoka, S. Kambe, Y. Itoh, and T. Machi, Physica B **199&200**, 278 (1994).

<sup>9</sup>A. A. Gippius, E. V. Antipov, W. Hoffmann, and K. Lüders, Physica C **276**, 57 (1997).

<sup>10</sup>V. A. Alyoshin, D. A. Mikhailova, and E. V. Antipov, Physica C **255**, 173 (1995).

<sup>11</sup>S. M. Loureiro, E. T. Alexandre, E. V. Antipov, J. J. Capponi, S. de Brion, B. Souletie, J. L. Tholence, M. Marezio, Q. Huang, and A. Santoro, Physica C **243**, 1 (1995).

<sup>12</sup>M. Karppinen, A. Fukuoka, L. Niinistö, and H. Yamauchi, Supercond. Sci. Technol. **9**, 121 (1996).

<sup>13</sup>*NMR Frequency Table*, Bruker Almanac (Bruker GmbH, Karlsruhe, 1992).

<sup>14</sup>B. J. Suh, F. Borsa, Ming Xu, D. R. Torgeson, W. J. Zhu, Y. Z. Huang, and Z. X. Zhao, Phys. Rev. B **50**, 651 (1994).

<sup>15</sup>M. Horvatić, C. Berthier, P. Caretta, J. A. Gillet, P. Ségransan, Y. Berthier, and J. J. Capponi, Physica C **235-240**, 1669 (1994).

<sup>16</sup>B. J. Suh, F. Borsa, J. Sok, D. R. Torgenson, Ming Xu, Q. Xiong, and C. W. Chu, Phys. Rev. B **54**, 545 (1996).

<sup>17</sup>M. Mehring, Appl. Magn. Reson. **3**, 383 (1992).

<sup>18</sup>M. Horvatić, T. Auler, C. Berthier, Y. Berthier, P. Butaud, W. G. Clark, J. A. Gillet, P. Ségransan, and J. Y. Henry, Phys. Rev. B **47**, 3461 (1993).

<sup>19</sup>M.-H. Julien, M. Horvatić, P. Caretta, C. Berthier, Y. Berthier, P. Ségransan, S. M. Loureiro, and J.-J. Capponi, Physica C **268**, 197 (1996).

<sup>20</sup>J. F. Banger, P. C. Taylor, T. Oja, and P. J. Bray, J. Chem. Phys. **50**, 4914 (1969).

<sup>21</sup>D. E. Farnell, B. S. Chandrasekhar, M. R. DeGuire, M. M. Fang, V. G. Kogan, J. R. Clem, and D. K. Finnemore, Phys. Rev. B **36**, 4025 (1987).

<sup>22</sup>K. Yosida, Phys. Rev. **110**, 769 (1958).

<sup>23</sup>D. Brinkmann and M. Mali, *NMR-NQR Studies of High-Temperature Superconductors*, Vol. 31 of *NMR Basic Principles and Progress* (Springer Verlag, Berlin, 1994).

<sup>24</sup>F. Borsa, P. Carreta, M. Corti, and A. Rigamonti, Appl. Magn. Reson. **3**, 509 (1992).

<sup>25</sup>C. Pennington and C. P. Slichter, Phys. Rev. Lett. **66**, 381 (1991).

<sup>26</sup>F. Mila and T. M. Rice, Physica C **157**, 561 (1989).

<sup>27</sup>H. Monien and D. Pines, Phys. Rev. B **41**, 6297 (1990).

<sup>28</sup>N. Bulut and D. J. Scalapino, Phys. Rev. B **45**, 2371 (1992).

<sup>29</sup>D. Thelen, D. Pines, and Jian Ping Lu, Phys. Rev. B **47**, 9151 (1993).

<sup>30</sup>N. Bulut, D. W. Hone, D. J. Scalapino, and N. E. Bickers, Phys. Rev. B **41**, 1797 (1990).

<sup>31</sup>A. J. Millis, H. Monien, and D. Pines, Phys. Rev. B **42**, 167 (1990).

<sup>32</sup>Z.-X. Shen, D. S. Dessau, B. O. Wells, D. M. King, W. E. Spicer, A. J. Arko, D. Marshall, L. M. Lombardo, A. Kapitulnik, P. Dickinson, S. Doniach, J. DiCarlo, A. G. Loeser, and C. H. Park, Phys. Rev. Lett. **70**, 1553 (1993).